

## Phase developments and dielectric responses of barium substituted four-layer $\text{CaBi}_4\text{Ti}_4\text{O}_{15}$ Aurivillius

HUILING DU\*, XIANG SHI and HUILU LI

College of Materials Science and Engineering, Xi'an University of Science and Technology, Xi'an 710054, China

MS received 26 December 2010; revised 8 February 2011

**Abstract.** In this paper, mixed Ca–Ba oxide  $\text{Ca}_{1-x}\text{Ba}_x\text{Bi}_4\text{Ti}_4\text{O}_{15}$  (CBBT) ceramics, fabricated by the improved traditional ceramics process were investigated by doping concentrations of Ba ion up to  $x = 0.9$  (in steps of 0.1). At room temperature, an orthorhombic crystal system was confirmed using XRD, and their parameter was obtained using the Rietveld method. Dielectric properties and phase transitions were studied and are explained in terms of lattice response of these ceramics. A shift in ferroelectric–paraelectric phase transition ( $T_C$ ) to lower temperatures and a corresponding decrease in permittivity peak with increasing concentration of  $\text{Ba}^{2+}$  are also observed. The ferroelectric–paraelectric phase transition of CBBT compounds is of normal type in nature, differing from the relaxor characteristic of BBT. The decrease of orthorhombicity in the lattice structure by the larger  $\text{Ba}^{2+}$  ion incorporation, indicating an approach of  $a$  and  $b$ , results in lower Curie temperature. Appearance of anomalous loss peaks of Ba-rich compounds at  $530^\circ\text{C}$  reveals a phase transition development trend from ferroelectric orthorhombic structure to the paraelectric orthorhombic structure. Relationship of polarization with lattice response is discussed.

**Keywords.** Aurivillius; substitution; orthorhombic distortion; phase transition.

### 1. Introduction

Lead-based piezoelectric ceramics have dominated the commercial market for the past several years, owing to their outstanding piezoelectric, dielectric, ferroelectric and electromechanical properties. However, the toxicity of lead has raised concerns about lead-based piezoelectric materials. Therefore, lead-free functional materials are highly desirable for environment-friendly applications.

Large remnant polarization, low coercive field, and high Curie temperature are required for better performance and reliable operations of FRAM devices. Aurivillius-type BLSFs received significant attention for their potential use in non-volatile ferroelectric random-access memory and high-temperature piezoelectric devices, owing to their fatigue-free properties and their relatively high Curie temperature,  $T_C$ , respectively. Since bismuth layered structure ferroelectrics play an important role in the dielectric and ferroelectric devices, its crystal structure and material properties have been widely investigated for the past several decades (Saito *et al* 2004; Karthik *et al* 2006; Wang *et al* 2009). Aurivillius oxides can be described as regular stacking of  $[\text{A}_{n-1}\text{B}_n\text{O}_{3n+1}]^{2-}$  perovskite blocks, separated by fluorite like  $(\text{Bi}_2\text{O}_2)^{2+}$  layers. The perovskite blocks offer large possibilities in terms of compositional flexibility, which allows incorporation of various cations such as  $\text{Na}^+$ ,  $\text{K}^+$ ,  $\text{Ca}^{2+}$ ,

$\text{Sr}^{2+}$ ,  $\text{Ba}^{2+}$ ,  $\text{Pb}^{2+}$ , or  $\text{Ln}^{3+}$  in the  $A$ -site and  $\text{Fe}^{3+}$ ,  $\text{Cr}^{3+}$ ,  $\text{Ti}^{4+}$ ,  $\text{Nb}^{5+}$  or  $\text{W}^{6+}$  in the  $B$ -site. It is thus possible to modify the dielectric and ferroelectric properties by changing the chemical composition. The effect of  $A$ -site substitution is more obvious than that of  $B$ -site substitution, since the cations in  $B$  sites are similar in size and do not play a major structural role in the polarization process for BLSFs (Jannet *et al* 2003; Sun *et al* 2008; Rout *et al* 2009). Recently, crystallographic studies have demonstrated the key role of the  $A$ -site cation in the ferroelectric behaviour of these materials (Remondiere *et al* 2006; Tellier *et al* 2007; Coondoo *et al* 2009). Thus direct relations among the average ionic radii of the  $A$ -site cation, chemical bonding, and Curie temperature ( $T_C$ ) could be established in ferroelectric Aurivillius oxides.

Recently, these bismuth layer-structured materials have been intensively investigated as lead-free ferroelectric and piezoelectric materials.  $\text{CaBi}_4\text{Ti}_4\text{O}_{15}$  (CBT) and  $\text{BaBi}_4\text{Ti}_4\text{O}_{15}$  (BBT) are interesting in the sense that they represent two limit cases considering the average ionic radii of the  $A$ -site cation in Aurivillius oxides.  $\text{CaBi}_4\text{Ti}_4\text{O}_{15}$ , with space group of  $A2_1am$ , could be regarded as a representative example of a 'classic' Aurivillius ferroelectric phase while  $\text{BaBi}_4\text{Ti}_4\text{O}_{15}$  exhibits a relaxor behaviour.  $\text{CaBi}_4\text{Ti}_4\text{O}_{15}$  is a very promising candidate for high temperature piezoelectric applications due to its high Curie temperature ( $790^\circ\text{C}$ ) and excellent retention characteristics. Attempts have been made to introduce the orthorhombic distortion in CBT ceramic after incorporating dopant in the lattice. The presence of orthorhombic distortion was reported to enhance the piezoelectric and ferroelectric properties of modified CBT

\* Author for correspondence (hldu@xust.edu.cn)

ceramics (Kennedy *et al* 2003; Suzuki *et al* 2006; Wang *et al* 2008; Tanwar *et al* 2009).

In order to investigate in finer detail for a certain limit of  $\text{Ba}^{2+}$  that can be introduced into CBT and provide materials with good electrical characteristics, a series of ceramics with the same formula,  $\text{Ca}_{1-x}\text{Ba}_x\text{Bi}_4\text{Ti}_4\text{O}_{15}$  ( $x = 0.1, 0.2, 0.3, 0.4, 0.6, 0.7, 0.8, 0.9$ ) (CBBT100 $\times$ ), were fabricated by the improved traditional ceramics process with cold-isostatic pressing. Influence of  $\text{Ba}^{2+}$  content on microstructure, phase developments and dielectric behaviours of CBBT100 $\times$  ceramics was determined and discussed.

## 2. Experimental

The polycrystalline samples of  $\text{Ca}_{1-x}\text{Ba}_x\text{Bi}_4\text{Ti}_4\text{O}_{15}$  (CBBT) ceramics with  $x = 0-0.9$  were prepared by solid state reaction method. The used starting materials were bismuth oxide ( $\text{Bi}_2\text{O}_3$ ), calcium carbonate ( $\text{Ca}_2\text{CO}_3$ ), titanium oxide ( $\text{TiO}_2$ ) and barium carbonate ( $\text{BaCO}_3$ ), all of analytical grade. The powders were mixed with a desired weight ratio and ball-milled in ethanol with zirconia balls for 5 h followed by calcination at 800–850°C for 2 h in an alumina crucible. The ground calcinated powders were ball-milled again for 5 h and dried. After uniaxially pressing into pellets, the pellets were cold isostatic pressed at 200 MPa for 20 min to obtain the homogeneous and better compaction of green specimens. After burning out the PVA at 550°C for 5 h, the green compacts were fully surrounded by the powder of matching compositions in a closed alumina crucible and sintered at 1100–1200°C for 2 h. Finally, relative density for the final

ceramic, measured by Archimedes method, was found to be above 96%.

The structure of CBBT100 $\times$  ceramic powder was determined by XRD analysis, using a Rigaku D/max 2500v PC X-ray diffractometer with Cu  $K\alpha$  radiation. The microstructure evolution was observed using a scanning electron microscopy (JSM 6460LV, Japan). Fired-on silver paste was used as the electrode for measurement of electrical properties. Dielectric measurements were carried out using a computer controlled Agilent 4284A LCR meter in a wide frequency (1 kHz to 1 MHz) and temperature range (25–700°C).

## 3. Results and discussion

Figure 1 shows the room temperature XRD patterns of all the calcined CBBT powders. Referencing the improvement in the structure investigation of four Aurivillius phases, CBT and BBT adopt an orthorhombic structure at room temperature and the structures have been refined in a space group  $A2_1am$ . Compared with the pattern of pure CBT and BBT ceramics, the CBBT are also bismuth layer-structured ferroelectrics with  $m = 4$ . Analysis of the patterns confirmed that all samples have orthorhombic symmetry. The peak associated with the (119) plane has the highest intensity, indicating that the ceramics have a bismuth layered structure with  $m = 4$ . It has been shown that the most intense diffraction peaks of BLSF are all of the type  $(112m+1)$ . With the increase of  $x$ , the diffraction peak positions move to lower angles, because of an increase in the cell size with increasing  $x$ .

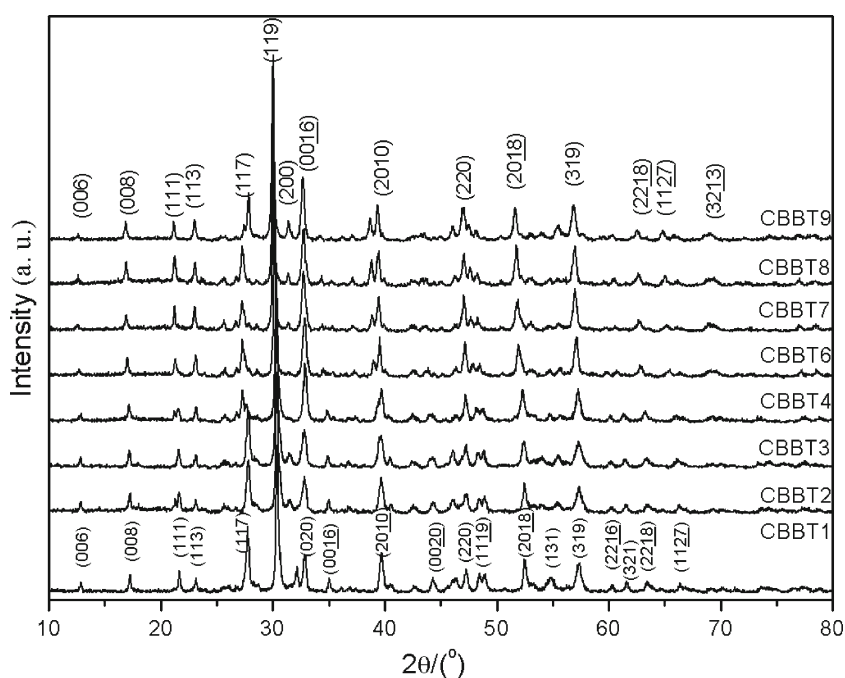


**Figure 1.** X-ray diffraction patterns of calcined  $\text{Ca}_{1-x}\text{Ba}_x\text{Bi}_4\text{Ti}_4\text{O}_{15}$  (CBBT100 $\times$ ) powders.

Some variation in the intensities of peaks and shifts in the positions of certain peaks have been observed which can be attributed to the variation in lattice distortions in the samples. Lattice parameters, shown in table 1, are calculated from the obtained  $d$ -values and are used to calculate structural distortion parameters such as orthorhombic distortion, which can be quantified as  $2(a - b)/(a + b)$ . The replacement of  $\text{Ca}^{2+}$  by  $\text{Ba}^{2+}$  leads to the volume expansion, with predominantly elongating along the  $c$ -axis rather than  $a$ - and  $b$ -directions. Compared to the 3.5% expansion from CBBT1 to CBBT9, the expansion in the  $a$  and  $b$  directions is noticeably less, 0.8% and 0.2%, respectively. A decrease in orthorhombicity in the lattice structure of CBBT was seen with an increase in  $\text{Ba}^{2+}$  doping. The value of orthorhombicity rapidly decreases from 0.0087 for CBBT1 to 0.00031 for CBBT9, indicating less orthorhombic structure distortion

with  $\text{Ba}^{2+}$  substitution. Tellier *et al* (2004) also presented selected area electron diffraction data to support that the tilting of the octahedra are much smaller in BBT compared to CBT and  $\text{SrBi}_4\text{Ti}_4\text{O}_{15}$  (SBT).

SEM micrographs of as-fired surfaces of CBBT ceramics were obtained and are shown in figure 2. It can be seen that the ceramics have a dense structure and plate-like morphology. This plate-like morphology of the grain is a characteristic feature of bismuth layer compounds. The plate-like crystal grains for Ca-rich composition are much thinner than that of Ba-rich composition. Due to the high grain growth rate in the direction perpendicular to the  $c$ -axis of the BLSFs crystal, the grain growth is structurally highly anisotropic. Horn also reported that the (00 $l$ ) plane of the Aurivillius structure possesses lower surface energies which develop predominantly during sintering (Horn *et al* 1999). Thus plate-like grains

**Table 1.** Crystal structural parameters of CBBT100 $\times$  oxides.

CBBT $_x$	CBBT1	CBBT2	CBBT3	CBBT4	CBBT6	CBBT7	CBBT8	CBBT9
$t$	0.960	0.964	0.967	0.970	0.977	0.980	0.983	0.987
$V$	1241.721	1238.448	1236.528	1199.038	1200.203	1206.747	1214.834	1226.123
$b/a$	1.0087	1.0061	1.0044	1.0037	1.0021	1.0019	1.0018	1.0009
$2(a - b) / (a + b) \times 10^{-3}$	8.70	6.03	4.41	3.67	2.07	1.89	1.76	0.31

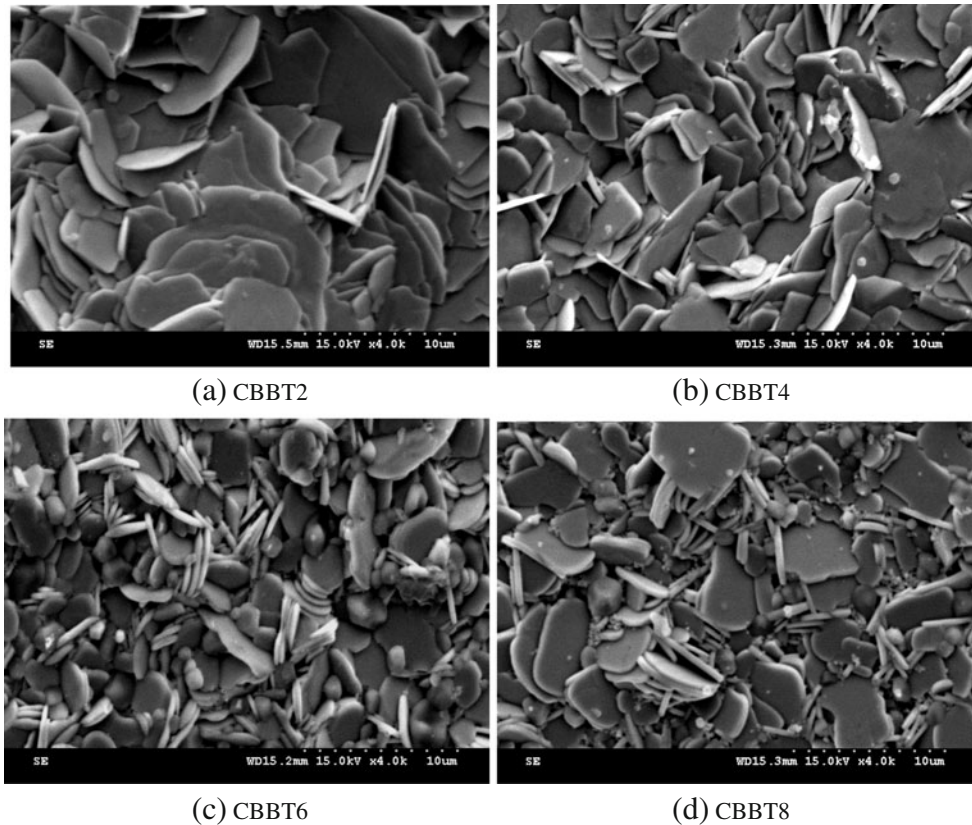


**Figure 2.** SEM micrographs of natural surface of CBBT ceramics.

(with the  $c$ -axis oriented normal to the flat surface of the grains) are formed in the ceramics. However, as the ceramics are fabricated by pressure-less sintering, the orientation of the plate-like grains is random. It is also noted that, after doping of  $\text{Ba}^{2+}$ , the grains become smaller. With increasing  $\text{Ba}^{2+}$  content there is a small increase in the 'thickness' of plate-like grains as compared with the significant decrease in the 'width'. The thickness/length ratio of the plate-like grain is much bigger for Ca-rich compounds than that of Ba-rich compounds.

The replacement of  $\text{Ca}^{2+}$  by  $\text{Ba}^{2+}$  leads to the chemical formation of impurities and defects, which have a profound influence on the static and dynamic properties of this material. The dielectric properties of CBBT ceramics were studied and are as shown in figure 3. Room temperature dielectric constant value increases from 135 for CBBT1 to 182 for CBBT9 gradually, while dielectric loss reduces significantly with  $\text{Ba}^{2+}$  doping. This result probably could be understood by considering the fact that dielectric permittivity is mainly related to ionic polarizability, which is closely related to structural displacement distortion. The increase in permittivity is most likely linked to the replacement of lower polarizable  $\text{Ca}^{2+}$  cations with highly polarizable  $\text{Ba}^{2+}$ . The higher value of permittivity is possibly due to the enhanced polarizability of the host ions and the strong interaction between the dipole moments in the layered structure. Similar observation of enhanced dielectric permittivity with  $\text{Ba}^{2+}$  doping in  $\text{PbBi}_2\text{Nb}_2\text{O}_9$  has also been reported recently (Du *et al* 2008).

Figure 4 shows variation of dielectric permittivity as a function of temperature at 10 kHz. No phase transition peak was observed for Ca-rich compounds ( $x \leq 0.4$ ) within the measured temperature range (up to  $700^\circ\text{C}$ ), indicating the Curie temperature  $T_C$  of those compositions is above  $700^\circ\text{C}$ .

It is shown that permittivity peak observed only for Ba-rich compounds ( $x > 0.5$ ), gradually decreases from  $594^\circ\text{C}$  (for CBBT6) to  $498^\circ\text{C}$  for CBBT9. The magnitude of the dielectric constant decreases rapidly with an increase in frequency, but no significant frequency shifts for temperature corresponding to the maximum of dielectric permittivity ( $T_m$ ). Above the transition temperature, permittivity follows the Curie–Weiss law. Compared to  $\text{BaBi}_4\text{Ti}_4\text{O}_{15}$ , which shows a broad phase transition around  $420^\circ\text{C}$ , all CBBT ceramics present a normal paraelectric–ferroelectric phase transition at much higher temperatures (Pribošič *et al* 2001). We note that there is no significant frequency dispersion of permittivity peak even for CBBT9. This indicates that the ferroelectric–paraelectric phase transition of CBBT compounds is of normal type in nature, differing from the relaxor characteristic of BBT.

The tangent losses as a function of temperature at 1 kHz for CBBT are shown in figure 5. The appearance of two dielectric loss peaks in Ba-rich compounds (where  $x > 0.5$ ) is different from the dielectric loss measurement in Ca-rich samples (where  $x < 0.5$ ), where only one apparent dielectric loss peak was observed. Figure 6 shows the temperature dependence of the dielectric constant and loss of CBBT7 and CBBT9 in the temperature range from  $300$ – $650^\circ\text{C}$ . Even for CBBT9, no apparent frequency dispersion of dielectric constant is observed, although  $\epsilon_m$  decreases rapidly with the increase in frequency. For CBBT9, the  $T_m$  shifting with frequency is much smaller than in BBT ceramics in the frequency range between 1 kHz and 1 MHz (Kennedy *et al* 2003). It is also noticed that there is a small dielectric abnormality in dielectric loss of CBBT9 at about  $530^\circ\text{C}$ , which was also observed in other Ba-rich compounds (where  $x > 0.5$ ). We assume that this phenomenon should be attributed

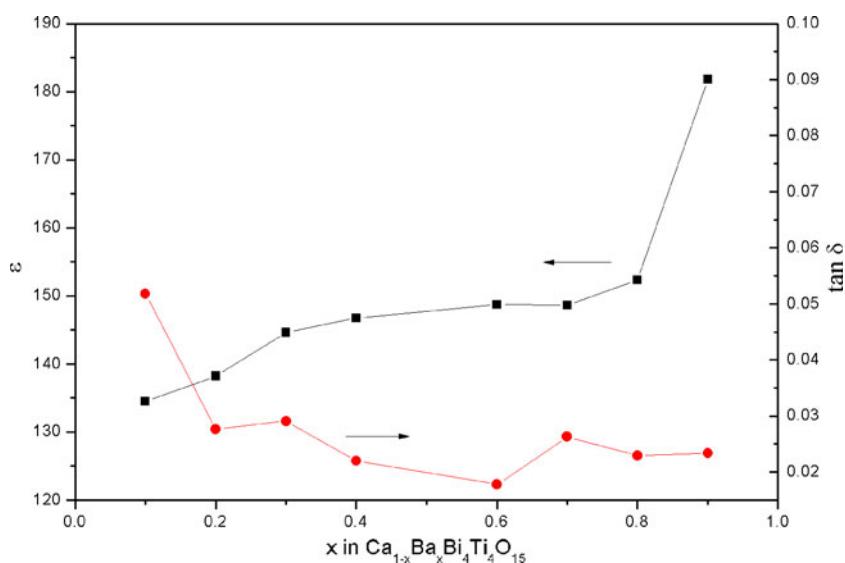


**Figure 3.** Composition dependence of dielectric permittivity and loss of CBBT at 1 kHz.

to the action of  $\text{Ca}^{2+}$ , which plays a leading role when  $x < 0.5$ . Therefore, CBBT could be thought of as  $\text{Ba}^{2+}$ -doped CBT when  $x < 0.5$ . Inversely, when  $x > 0.5$ , the CBBT could be considered as Ca-doped BBT and the  $\text{Ba}^{2+}$  plays a leading role, thus the phase transition mechanism appeared as a boundary when  $x$  was 0.5. At high Ba-rich compounds, a second weak anomaly in the dielectric loss as a function of temperature could be observed between 550 and 650°C which may be related to the phase transition to a paraelectric orthorhombic structure (*Amam*) for Ba-rich compounds. The group theoretical analysis of Macquart *et al* (2002) showed a continuous transition to *I4/mmm* as it must involve an

intermediate phase in the four-layer oxides. Kennedy *et al* (2008) observed there is an obvious discontinuity in the orthorhombic strain with temperature using a combination of synchrotron X-ray and neutron powder diffraction data in BBT, and that is possibly associated with a transition to a paraelectric orthorhombic structure. While for both CBT and SBT, the strains provide no evidence for such a transition. Considering the recent studies and our results, it is reasonable to approve that increasing the temperature would result in a transition first to a paraelectric *Amam* orthorhombic phase and ultimately to a tetragonal *I4/mmm* structure in Ba-rich compounds.

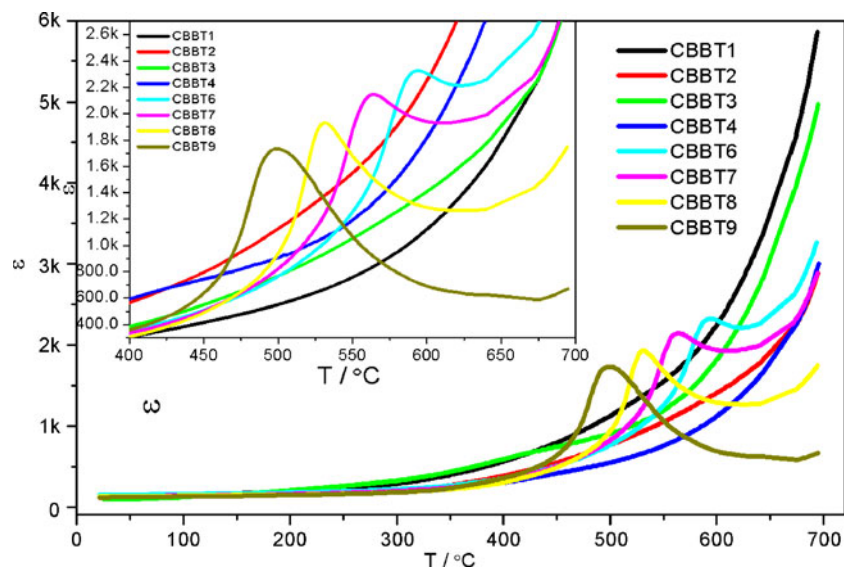


**Figure 4.** Temperature dependence of dielectric constant of CBBT ceramics at 10 kHz and inset shows an expanded view of permittivity peak between 400 and 700°C.

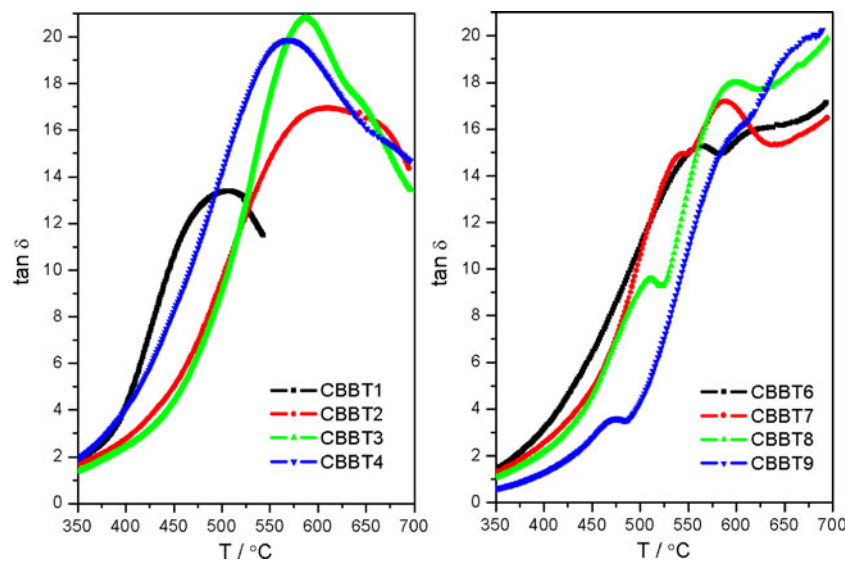


**Figure 5.** Temperature dependence of dielectric loss of CBBT ceramics at 10 kHz.

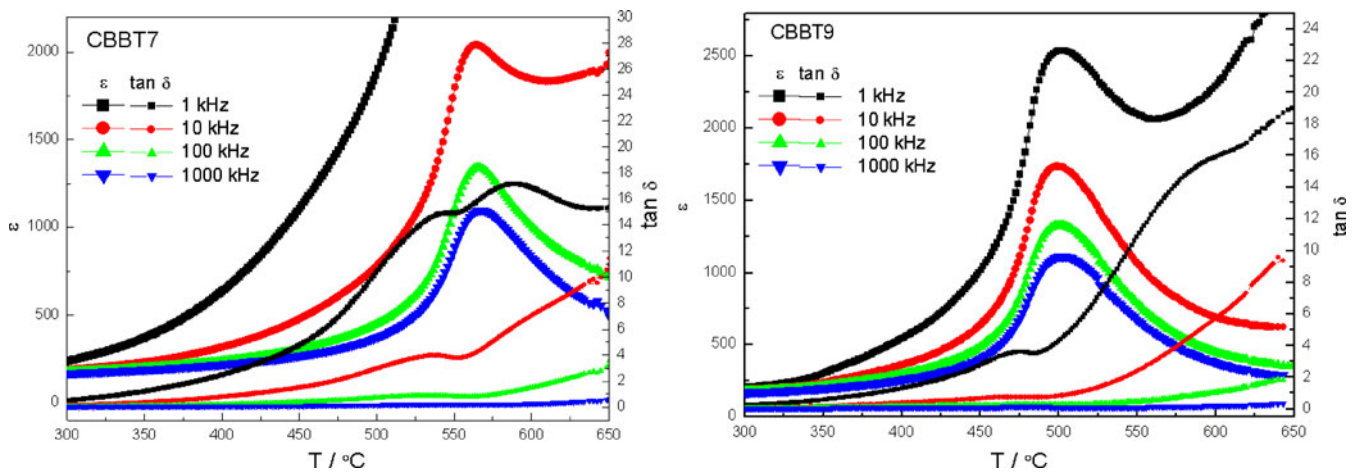


**Figure 6.** Temperature dependence of dielectric constant and dielectric loss of CBBT7 and CBBT9 at various frequencies.

Tangent losses increase with increasing temperatures particularly at temperatures higher than 400°C. This could be caused by a higher concentration of charge carriers at higher temperatures. The permittivity maximum, which coincides with the minimum of the dielectric loss, is significant of the onset of a close to second order ferroelectric to paraelectric phase transition. It is also noticed that with an increase in Ba<sup>2+</sup> doping, the tangent losses decrease, both at ambient temperature and high temperatures. This might be related to the increased complexity in the crystal structure via Ba<sup>2+</sup> doping.

In the Aurivillius structure compounds, the Curie temperature is always found associated with the structure distortion. The lower the Curie temperature, the less the orthorhombic distortion at room temperature. In this study, the orthorhombicity is 0.0087 for CBBT1, and its value decreases to 0.00031 for CBBT9, which indicates less orthorhombic structure distortion with the substitution. This is consistent with the lowering of Curie temperature. Moreover, usually ferroelectrics with a large ionic displacement have a high Curie temperature and a large spontaneous polarization. The ionic displacements are influenced by several factors including the ionic size, tolerance factor, and ionic polarizability. Considering the average ionic radii of the A site cation, the perovskite tolerance factors,  $t = \frac{R_A + R_O}{\sqrt{2}(R_B + R_O)}$ , are found to increase from 0.96 to 0.987 for CBBT1 to CBBT9, respectively. The decrease of Curie temperature ( $T_C$ ) and permittivity peak ( $\epsilon_{\text{max}}$ ) with increasing amount of Ba<sup>2+</sup> doping in the CBT compounds has been attributed to the increase of the tolerance factor, which leads to a less distorted structure ( $a$  and  $b$  parameters becoming close to one another). Accordingly, the atomic displacements along the polar axis ( $a$ -axis) are smaller so that the energy involved to reach the prototype high temperature structure is lowered. Moreover, the ionic radii and polarizability could have essential influences on ferroelectric

properties. The substitution of A-site Ca<sup>2+</sup> ion with larger radii Ba<sup>2+</sup> reduces the rattle space for B site ion, the replacement of lower polarizable Ca<sup>2+</sup> cations with highly polarizable Ba<sup>2+</sup> in compositions results in structural displacement distortion, all have contributions in lowering of  $T_C$ . Enhancing the size of A-type cation lowers the tilting of TiO<sub>6</sub> octahedra. This is consistent with the lowering of Curie temperature. Furthermore, in layer-structured perovskites, the crystal structure may not change as freely as that of perovskites with doping due to the structural constraint imposed by the (Bi<sub>2</sub>O<sub>2</sub>) interlayer. Thus the reduction of the rattling space between the octahedrons and the (Bi<sub>2</sub>O<sub>2</sub>) layer can induce a suppression of the Curie temperature.

#### 4. Conclusions

In this study, Ca<sub>1-x</sub>Ba<sub>x</sub>Bi<sub>4</sub>Ti<sub>4</sub>O<sub>15</sub> ceramics with doping concentrations of Ba<sup>2+</sup> up to  $x = 0.9$  (in steps of 0.1) were successfully prepared by the improved traditional ceramics process with cold-isostatic pressing. At room temperature, an orthorhombic crystal system was confirmed using XRD, and their parameter was obtained using the Rietveld method. The Ba<sup>2+</sup> doping has an effect of lowering the Curie temperature, suppressing the permittivity peak and repressing grain growth. Temperature dependent dielectric study showed normal ferroelectric to paraelectric transition well above 400°C for all studied compositions. It can be inferred that substitution of Ca by the larger cation Ba<sup>2+</sup> would lead to a lower thermal energy of phase transition, thus gradually decreasing the  $T_C$  from 594°C to 498°C for Ba-rich compounds. Calculated structure parameters show that enhancing the size of the A-type cation lowers the tilting of the TiO<sub>6</sub> octahedra. The decrease of the orthorhombic distortion further causes a decrease of the Curie temperature. Rather, it is proposed that the

mixed Ca–Ba oxide,  $\text{Ca}_{1-x}\text{Ba}_x\text{Bi}_4\text{Ti}_4\text{O}_{15}$ , is orthorhombic in  $A2_1am$  at room temperature, thus increasing the temperature results in a transition first to a paraelectric  $Amam$  orthorhombic phase and ultimately to a tetragonal  $I4/mmm$  structure for Ba-rich compounds.

### Acknowledgements

This work was supported by the Natural Science Foundation of China under grant no. 51072162 and the Science and Technology Development Plan Foundation of Shaanxi Province (2010K09-18).

### References

- Coondoo I, Agarwal S K and Jha A K 2009 *Mater. Res. Bull.* **44** 1288
- Du H L, Li Y, Li H L, Shi X and Liu C 2008 *Solid State Commun.* **148** 357
- Horn J A, Zhang S C, Selvaraj U, Messing G L and Trolier-McKinstry S 1999 *J. Am. Ceram. Soc.* **82** 921
- Jannet D B, El Maaoui M and Mercurio J P 2003 *J. Electroceram.* **11** 101
- Karthik C, Ravishankar N, Maglione M and Vondermuhl R 2006 *Appl. Phys. Lett.* **89** 042905
- Kennedy B J, Kubota Y, Hunter B A, Ismunandar and Kato K 2003 *Solid State Commun.* **126** 653
- Kennedy B J, Zhou Q D, Ismunandar, Kubota Y and Kato K 2008 *J. Solid State Chem.* **181** 1377
- Macquart R, Kennedy B J, Vogt T and Howard C J 2002 *Phys. Rev.* **B66** 2121021
- Pribošič I, Makovec D and Drogenik M 2001 *J. Euro. Ceram. Soc.* **21** 1327
- Remondiere F, Boullay P and Mercurio J P 2006 *Mater. Sci. Eng. B–Solid* **131** 235
- Rout S K, Sinha E, Hussain A, Lee J S, Ahn C W, Kim I W and Woo S I 2009 *J. Appl. Phys.* **105** 024105
- Saito Y, Takao H, Tani T, Nonoyama T, Takatori K, Homma T, Nagaya T and Nakamura M 2004 *Nature* **432** 84
- Sun J, Jin C and Chen X B 2008 *Integr. Ferroelectr.* **98** 77
- Suzuki T S, Kimura M, Shiratsuyu K, Ando A, Sakka Y and Sakabe Y 2006 *Appl. Phys. Lett.* **89** 132902
- Tanwar A, Sreenivas K and Gupta V 2009 *J. Appl. Phys.* **105** 084105
- Tellier J, Boullay Ph, Manier M and Mercurio D 2004 *J. Solid State Chem.* **177** 1829
- Tellier J, Boullay Ph, Ben Jennet D and Mercurio D 2007 *J. Eur. Ceram. Soc.* **27** 3687
- Wang C M, Wang J F, Zhang S J and Shrout T R 2009 *J. Appl. Phys.* **105** 094110
- Wang W, Shan D, Sun J B, Mao X Y and Chen X B 2008 *J. Appl. Phys.* **103** 044102